Validation of the One-Point Approach of the Elliptic Cone Model for the 13 December 2006 Frontside Full Halo Coronal Mass Ejection

X. P. Zhao

W. W. Hansen Experimental Physics Laboratory, Stanford University, USA

H. Cremades

Universidad Tecnologica Nacional / CONICET, Mendoza, Argentina

M. J. Owens [1]

Center for Space Physics, Boston University, Boston, Massachusetts, USA.

Short title: VALIDATION OF THE ELLIPTIC CONE MODEL

[1]Now at: Space and Atmospheric Physics, Imperial College London, Prince Consort Road, London SW7 2BZ, United Kingdom

Abstract. To invert the radial propagation speed and acceleration from the measured sky-plane speed and acceleration of frontside full-halo CMEs, an algorithm is developed on the basis of the elliptic cone model parameters. The elliptic cone model parameters for the 13 December 2006 frontside full halo CME are inverted using the one-point approach, i.e., using the halo CME image and the position of associated flare. In searching for the projection angle between the CME propagation direction and the plane of the sky, it is assumed for fast halo CMEs that the candidate projection angle should be located at the point on the α-curve [Zhao, 2008] that is the minimum distance from the flare position to the α-curve. We show that the observed elliptic halo can be well reproduced using the inverted model parameters; the inverted kinematic properties agree well with those determined by Type II observations; and the solar wind disturbances ahead of the ejection associated with the 13 December 2006 full-halo CME can also be well reproduced. The agreement between calculations and observations suggests that both the algorithm developed here for inverting the actual kinematic properties and the minimum-distance criterion used for determining the projection angle of the fast frontside full-halo CMEs are valid for fast frontside full-halo CMEs. It is also shown that the condition of the minor axis of the halo passing through the solar disk center is a necessary but not sufficient condition for using the circular cone model to invert actual geometrical and kinematical properties for frontside full-halo CMEs.

1. Introduction

Coronal mass ejections (CMEs) with apparent (i.e., sky-plane) angular width of 360° and associated with near-surface activity are defined as frontside full-halo (FFH) CMEs. FFH CMEs are mostly symmetric and ellipse-like. The geoeffectiveness rate of FFH CMEs is greater than 70%, reaching the higher end of the range of geoeffectiveness rate of all kinds of solar activities [Zhao and Webb, 2003; Gopalswamy, Yashiro, and Akiyama, 2007]. The knowledge of actual geometric and kinematic properties of 3-D CMEs which appear as 2-D FFH CMEs is essential for space weather forecasting. In this study, we address the issue of best invert the actual geometric and kinematic properties of 3-D CMEs from measured apparent geometric and kinematic properties of 2-D ellipse-like FFH CMEs on the plane of the sky (sky-plane).

Based on the observational fact that most limb CMEs propagate radially with constant angular width, a geometrical model for the 3-D CMEs was developed for inverting the actual geometric and kinematic properties of 3-D CMEs from observed 2-D FFH CMEs. This cone model, a hollow body which narrows to it's apex located at Sun's spherical center from a round, flat base [Zhao, Plunkett and Liu, 2002; Xie et al., 2004] is topologically similar to the conical shell model suggested by Howard et al. [1982] for understanding the formation of full-halo CMEs. The geometrical and kinematic properties obtained using the cone model for the 12 May 1997 FFH CME have been introduced at the boundary of a 3-D MHD solar wind model; and the arrival time at the Earth's orbit and the sheath structure ahead of the ICME have been successfully reproduced [Odstrcil, Riley and Zhao, 2004]. The success of the simulation indicates that the use of a cone-like geometric model to invert model parameters of 3-D CMEs from halo parameters of 2-D FFH CMEs is a valid means of estimating the actual geometrical and kinematic properties for FFH CME, which then may be used to launch CME structures at the inner boundary of MHD heliospherical models for numerically forecasting the space weather.

It was found, however, that cone model inversion is applicable to less than 10% of FFH CMEs because the semi-minor axis of the elliptic halos formed by the cone model must pass through solar disk center (See Figure 2 of Zhao et al., 2002 for details), which is not the case for the majority of events [Zhao, 2005; 2008].

With the aim of inverting the actual geometrical and kinematic properties of all kinds of elliptic FFH CMEs, a new cone-like model is developed. This elliptic cone model is defined as a hollow body which narrows to its apex located at Sun's center from an elliptic, flat base [Zhao, 2005; Cremades and Bothmer, 2005]. CMEs are believed to be driven by free magnetic energy stored in field-aligned electric currents, and before eruption, the metastable structure with free magnetic energy is confined by overlying arched field lines. The magnetic configuration of most, if not all, CMEs is thus expected to be magnetic flux ropes with two ends anchored on the solar surface (Riley et al., 2006). This kind of CME rope may be more correctly approximated by the elliptic cone model than the circular cone model since the outer edge of the top (or leading) portion of CME ropes appears more like an ellipse than a circle.

For the elliptic cone model, six model parameters are needed, three for the position of the base center, and three for the size, shape and orientation of the elliptic base (for the cone model, only four model parameters are necessary because only one parameter is needed to describe the circular base [Xie et al., 2004]). Observed elliptic halos, however, can provide only five halo parameters, two for the position of the halo center and three for the size, shape and orientation. It is thus difficult to uniquely determine six model parameters on the basis of five halo parameters [Cremades and Bothmer, 2005; Zhao, 2008].

We have established the equation system that relates model parameters with halo parameters, and presented two approaches, i.e. two-point and one-point approach, to uniquely find six model parameters [Zhao, 2008]. The present work will validate the one-point approach of the elliptic cone model using the well recognized, fast 13 December 2006 FFH CME. In what follows we first develop an algorithm for inverting the radial speed and acceleration on the basis of the measured sky-plane speed and acceleration at a measurement position angle. We then calculate geometrical and kinematic properties using five halo parameters and the position of the associated flare for the 2006 December 13 Disk FFH CME. To validate the one-point approach and newly established algorithm, we reproduce the observed FFH CME using inverted model parameters, compare the inverted speed with that from Type II observations, and compare the arrival time and the sheath structure ahead of the simulated ICME at Earth's orbit with in situ observations. Finally we summarize and discuss the results in the last section.

Figure 1.

2. The Algorithm for Determining the Radial Kinematic Property from the Sky-plane Kinematic Property

We work in the Heliocentric Ecliptic coordinate system $X_hY_hZ_h$ with X_h axis pointing to the Earth, Y_h axis to the west, and Z_h axis to the north, the plane Y_hZ_h denotes the plane of the sky. To express the orientation of an elliptic cone we introduce a coordinate system $X_cY_cZ_c$, with its origin colocated with the origin of the $X_hY_hZ_h$ system. Here X_c axis is aligned with the central axis of the elliptic cone (or the propagation direction of 3-D CMEs), and Y_c is the intersection between the plane Y_hZ_h and the plane Y_cZ_c normal to the X_c axis. Figure 1 shows the 13 December 2006 elliptic FFH CME on the Y_hZ_h plane and the definition and measured values of five halo parameters (SA_{xh}, SA_{yh}, D_{se}, α and ψ) for the CME.

The white ellipse enveloping the halo CME in Figure 1 is obtained using the 5-point method (See Cremades, 2005 for details). The X'_c axis is in the direction from solar disk center to the center of the white ellipse. It is the projection of the CME propagation direction X_c on the Y_hZ_h plane. Obviously, the Y'_c axis perpendicular to the X'_c axis must be aligned with the Y_c axis of the $X_cY_cZ_c$, system, which may be used to relate the orientation of elliptic cone bases, χ, to the orientation of elliptic halos, ψ (see Zhao, 2008 for the details). The CME propagation direction X_c is often expressed in ecliptic latitude λ and ecliptic longitude ϕ. In Equations below, we use the sky-plane latitude β and sky-plane longitude α to express the CME propagation direction X_c. Here parameter β is the projection angle between X_c and X'_c, and α, the azimuthal of the X'_c axis from the Y_h axis (see Figure 1). By using the projection angle β, the unknown model parameters are reduced to five from six, and the measured α may be helpful in determining the unknown β, as shown in next Section.

The white ellipse in Figure 1 can be reproduced by projecting the base of the elliptic cone first onto the Y_cZ_c plane with the angle χ from Y_eZ_e plane, then onto the $X_c'Y_c'$ plane with the angle β, and finally onto the Y_hZ_h plane with the angle α (See Zhao, 2008 for the detailed derivation). Thus we have

$$y_h = R_c\,p_y, \quad z_h = R_c\,p_z \tag{1}$$

$$\begin{aligned} p_y = {} & \cos\beta\cos\alpha + (\sin\beta\sin\chi\cos\alpha + \cos\chi\sin\alpha)\tan\omega_y\cos\delta_b - \\ & -(\sin\beta\cos\chi\cos\alpha - \sin\chi\sin\alpha)\tan\omega_z\sin\delta_b \end{aligned} \tag{2}$$

$$\begin{aligned} p_z = {} & -\cos\beta\sin\alpha - (\sin\beta\sin\chi\sin\alpha - \cos\chi\cos\alpha)\tan\omega_y\cos\delta_b + \\ & +(\sin\beta\cos\chi\sin\alpha + \sin\chi\cos\alpha)\tan\omega_z\sin\delta_b \end{aligned} \tag{3}$$

Where R_c is the distance from Sun's spherical center to the center of the cone base; ω_y and ω_z are the half angular width corresponding to the semi-axes of the elliptic base, SA_{yb} and SA_{zb} respectively; and χ is the angle between the semi-axis SA_{yb} of the elliptic cone base and the Y_c axis. The variable δ_b is the angular distance of elliptic base radii from semi-axis SA_{yb} or Y_e axis, and increases clockwise along the edge of the elliptic base from 0° to 360°.

Except R_c, all parameters in Equations (1)–(3) are assumed to be time-independent. The time-variation of y_h and z_h depends on the time-variation of R_c alone. The sky-plane speed and acceleration of halo CMEs are determined using height-time plots of the CMEs, and the CME heights are measured with respect to the disk center. Setting $R_{es} = \sqrt{y_h^2 + z_h^2}$, the measured sky-plane speed and acceleration at edge, V_{es} and a_{es}, can be calculated

$$V_{es} = \frac{dR_{es}}{dt}, \quad a_{es} = \frac{d^2 R_{es}}{dt^2}$$

and the radial speed and acceleration at the center of the elliptic cone base are

$$V_{cr} = \frac{dR_c}{dt} = \frac{V_{es}}{\sqrt{p_y^2 + p_z^2}}, \tag{4}$$

$$a_{cr} = \frac{d^2 R_c}{dt^2} = \frac{a_{es}}{\sqrt{p_y^2 + p_z^2}} \tag{5}$$

The radial speed and acceleration at the edge, V_{er} and a_{er} will be

$$V_{er} = V_{cr}/\cos\omega_e, \quad a_{er} = a_{cr}/\cos\omega_e \tag{6}$$

where the half angular width, ω_e, at δ_b can be calculated using model parameters ω_y and ω_z,

$$\cos\omega_e = \frac{1}{\sqrt{1 + \tan^2\omega_y \cos^2\delta_b + \tan^2\omega_z \sin^2\delta_b}} \tag{7}$$

Equation (7) shows that $\omega_e = \omega$ when $\omega_y = \omega_z = \omega$, indicating that the cone model is just a specific case of the more general elliptic cone model.

3. Determination of Actual Geometrical and Kinematical Properties for the 13 December 2006 FFH CME

Equations (1) – (7) show that given the sky-plane speed and acceleration of a FFH CME, V_{es} and a_{es}, at an edge point of δ_b, the radial speed and acceleration at the center and edge of the elliptic cone base, V_{cr}, a_{cr} and V_{er}, a_{er} can be inverted if the CME propagation direction (β, α), the elliptic cone base orientation, χ, and the half angular widths (ω_y and ω_z) are given.

3.1. Inversion of Model Parameters from Halo Parameters

To invert the model parameters β, χ, ω_y and ω_z from the halo parameters, we use the inversion equation system of model parameters [Zhao, 2008]

$$\begin{aligned} R_c &= D_{se}/\cos\beta \\ \tan\omega_y &= [-(a - c\sin\beta) + \sqrt{(a + c\sin\beta)^2 + 4\sin\beta\, b^2}\,]/(2R_c\sin\beta) \\ \tan\chi &= (R_c\tan\omega_y - c)/b \\ \tan\omega_z &= -(a + b\,\tan\chi)/R_c\sin\beta \end{aligned} \tag{8}$$

where

$$\begin{aligned} a &= SA_{xh}\cos^2\psi - SA_{yh}\sin^2\psi \\ b &= (SA_{xh} + SA_{yh})\sin\psi\cos\psi \\ c &= -SA_{xh}\sin^2\psi + SA_{yh}\cos^2\psi \end{aligned} \tag{9}$$

Equation systems (8) and (9) show that the four unknown model parameters, R_c, ω_y, ω_z and χ, can be uniquely determined from the four given halo parameters, D_{se}, SA_{xh}, SA_{yh} and ψ, if the projection angle β can be specified.

The candidate CME propagation direction may be, in general, at any λ and any ϕ. The relationship between the sky-plane latitude and longitude, β and α, and the ecliptic latitude and longitude, λ and ϕ, is

$$\sin\lambda = \cos\beta\sin\alpha, \qquad \tan\phi = \cos\alpha/\tan\beta \tag{10}$$

$$\sin\beta = \cos\lambda\cos\phi, \qquad \tan\alpha = \tan\lambda/\sin\phi \tag{11}$$

Equations (10) and (11) show that for a specific value of α, the candidate directions reduce to pairs of (λ, ϕ) that correspond to all possible β values. The curve in Figure 2 corresponds to $\alpha = 55.9°$, and is obtained by assuming that the possible values of β range from 45° to 90° for this disk FFH CME located within 45° of disk center.

Figure 2.

To select the candidate β from all possible points on the α-curve, we use the position of the flare associated with the FFH CME. The dark dot in Figure 2 denotes the flare position. It should be noted that the flare position is often specified using the latitude and longitude measured in the heliographic coordinate system, as shown by ϕ_{fs}, λ_{fs} in Figure 2. By correcting the effect of B0 angle (the heliographic latitude of the Earth) the flare position in the heliocentric ecliptic coordinate system, i.e., ϕ_{fe}, λ_{fe} in Figure 2, can be obtained.

CME-associated flares or active regions are often assumed to be located near the center of CME source region, and used to represent the CME propagation direction [e.g., Smith et al., 2008]. The dark dot would be located on the α-curve if it is the case. The deviation of the flare position from the α-curve, as shown in Figure 2, has been attributed to the effect of interaction between high-speed coronal hole streams and the propagating CMEs [e.g., Cremades et al., 2006]. For such fast CMEs as the 13 December 2006 FFH CME with the linear sky-plane speed of 1774 km/s, the effect of stream-CME interaction on the CME propagation direction can be neglected. Observations have shown that associated flares are often located near one leg of limb CMEs [e,g., Plunkett et al., 2001]. Therefore, we select the candidate β among all possible β on the α-curve by assuming that the candidate β should be located at the point on the α-curve which minimizes the distance between the dot and the α-curve. The obtained β (or ϕ_{ce}, λ_{ce}) is shown in Figure 2.

Once the candidate projection angle β is determined, other model parameters can be inverted, as shown in Table 1. **Table 1.**

As shown in Figure 1, the angle $\psi = 5.81°$, and $SA_{xh} < SA_{yh}$, indicates that the semi-minor axis of the 13 December 2006 FFH CME nearly passes through the solar disk center, suggesting that the FFH CME might be formed by the projection of a circular cone base on the sky-plane, and the geometrical properties of the 3-D CME rope may be uniquely inverted by the cone model. To compare the β values obtained from the two models and to see whether or not the condition of the halo's semi-minor axis passing through the solar disk center is a sufficient condition for using the cone model to invert model parameters, we calculate the four cone model parameters using the four halo parameters SA_{xh}, SA_{yh}, D_{se} and α, as shown in Table 1. It is expected that the two sets of model parameters should be the same if the cone base is circular. Table 1 shows that the model parameters inverted by the cone model are significantly different from that by the elliptic cone model. To compare the results with observations, the kinematical properties of the event are needed.

3.2. Calculation of the Actual Kinematic Properties

As shown in http://cdaw.gsfc.nasa.gov/CME_list/, for the 13 December 2006 FFH CME, the linear sky-plane speed at the measurement position angle (MPA) of 193° is 1774 km/s; the acceleration is -61.4 m/s^2, and the second order speed at the time of 2006/12/13_02:54:04 when the FFH CME shown in Figure 1 was observed is 1930 km/s. The MPA is defined counter clockwise from solar north in LASCO sky-plane, meaning

$$MPA = \tan^{-1}(-y_h/z_h) = \tan^{-1}(-p_y/p_z) \tag{12}$$

Thus the MPA depends on not only δ_b but also the five model parameters, ω_y, ω_z, χ, β and α. Using the five model parameters listed in Table 1 and the given value of MPA, we can determine the variable δ_b (see Table 1). Using Equations (2) – (7) and the model parameters shown in Table 1 the linear radial CME propagation speed at the edge of the elliptic cone base, V_{er1}, the second order radial propagation speed at 2006/12/13_02:54:04, V_{er2}, and the acceleration, a_{er}, can be calculated (See Table 1). To compare such obtained radial speeds with the estimate from Type II observations and with the MHD simulations, the second order radial propagation speed near the solar surface, $V_{er2_{01}}$, and at the 30 solar radii (the helipspheric base), $V_{er2_{30}}$, are also calculated (See Table 1).

Figure 3.

4. Validation of the Inversion Solution

The calculations of the elliptic cone model by one-point approach made in Section 3 for inverting actual geometrical and kinematic properties of the 13 December 2006 FFH CME are based on the assumption that the candidate β should be located at the point on the α-curve at the minimum distance between the flare position and the α-curve. The obtained β and other parameters are different from those of the cone model (See Table 1). In the following sections we attempt to determine which set of parameters provides the most valid solution.

4.1. Test of the inverted geometrical property

By substituting the two sets of model parameters into Equations (1)–(3) we obtain the two modeled halos. The red dashed (green dotted) ellipse in Figure 3 is produced by the elliptic (circular) cone model parameters. Both ellipses agree well with the white ellipse, indicating that Equations (1) – (3) and (8) – (11) that are used in the calculations are valid. It also shows that this kind of agreement is not a solid argument for the validation of the candidate β, though the red ellipse matches the white one slightly better than the green one.

4.2. Test of the inverted kinematical property

By using Type II observations, the radial propagation speed near the solar surface for the 13 December 2006 event has been estimated to be 2212 km/s [Liu et al., 2008]. The radial CME speed near the solar surface inverted by the elliptic cone model is 2323

km/s, agrees with the Type II estimate slightly better than the radial CME speed of 1997 km/s by the circular cone model. Furthermore, we have deduced the propagation speed of the CME's shock about half way its journey to Earth using Type II radio emissions in the kilometric domain. At those low frequencies it may be assumed that the CME's shock responsible for the emission has already undergone deceleration and that it is travelling at an approximately constant speed. The deduced speed near 120 solar radii from the Sun yielded V_{r120}= 1320 km/s, which should be less than the radial CME speed at 30 solar radii for the fast CME. The radial CME speed at 30 solar radii inverted using the elliptic cone model is 1585 km/s, greater than V_{r120}, but that inverted using the circular cone model is 1292 km/s, slightly less than V_{r120}. Thus Type II radio emissions further support the elliptic cone model.

4.3. Test of inverted geometrical and kinematical properties

To reconstruct the near-Earth solar wind disturbance caused by the 13 December 2006 FFH CME, we first use the "CORHEL" coupled 3-D magnetohydrodynamic (MHD) models of the corona-heliosphere system to simulate the ambient solar wind [Odstrcil et al., 2004a]. The corona in CORHEL is simulated by the SAIC "MHD Around a Sphere" (MAS) model [Linker et al., 1999; Mikic et al., 1999], which solves the time-dependent 3-D MHD equations using magnetograms as the inner boundary condition. At 30 solar radii, output from MAS is used as the inner boundary for the NOAA Space Weather Prediction Center (SWPC) "Enlil" model of the heliosphere [Odstrcil , 2003, and references therein], which solves the MHD equations on a Sun-centered spherical grid out to 2AU. This coupled scheme has been shown to match the bulk properties of the ambient solar wind very well [Owens et al., 2008].

Once the ambient solar wind conditions have been simulated, an overpressured density cloud is inserted at 30 Rs as a proxy for the transient disturbance resulting from the FFH CME. The cloud is assumed to be a spherical pulse, four times more dense and at the same temperature as the ambient solar wind. It does not contain an intrinsic magnetic field [Odstrcil et al., 2004b]. The CME velocity, angular width and the arrival time at 30 Rs can be specified by the circular or elliptic cone model fits to the coronagraph observations of FFH CMEs [Zhao et al., 2002; Zhao, 2008]. In this study, both the circular and elliptical cone model parameters are used to initialise the simulations, with the second order fits to the reconstructed height-time profile used to derive the time and speed at 30Rs: 1585 km/s at 05:28:13 UT (1217 km/s at 06:11:22) for the elliptical (circular) cone model . For the elliptical model, the width is set to be the average of the semi-major and semi-minor axes.

Figure 4 compares the ACE-observed near-Earth solar wind profile (black) with the simulated solar wind, initialised with the elliptical (red) and circular (blue) cone model parameters. In both cases, the disturbance arrives later than observed, which is expected due to the ambient solar wind simulation underestimating the wind upstream solar wind speed, and hence overestimating the drag force on the ejecta [Case et al., 2008]. The disturbance initiated with the elliptic cone model, however, is only 0.5-days late, compared to the 1-day error for the circular model. Both simulations produce the correct field and flow deflections in the sheath region ahead of the actual ejecta, suggesting the leading-edge orientation was correctly reproduced and thus supporting the geometric and kinematic properties inverted by the elliptic cone model. The body of the cloud is not expected to be reproduced, as the inner plasma and magnetic structure of the overpressured cloud is not realistic.

Figure 4.

5. Summary and Discussions

Based on the projection of the elliptic cone base on the plane of the sky, we have established the mathematical relationship between the apparent (sky-plane) speed and acceleration of frontside full-halo CMEs and the actual radial speed and acceleration of the 3-D CME ropes.

To invert the actual geometrical properties of the fast 13 December 2006 event we assume that the candidate projection angle β must be located at a specific point on the α-curve which minimizes the distance between the flare position and the α-cirve.

To invert the actual kinematic properties from observations, it is necessary to determine the relationship between the position angle of the measurement of the apparent speed and the variable δ_b, the angular distance of radii of the elliptic cone base from its semi-axis near the Y_c' axis. We establish Equation (12) that can be used to accurately determine the δ_b value that corresponds to the measurement position angle.

By using the elliptic cone model, the obtained actual geometrical and kinematic properties for the 13 December 2006 frontside full-halo CME have beed used to reproduce the observed halo CME, and to invert the radial propagation speed which agrees with the estimate of the radial propagation speed from Type II observations both near the Sun and near the Earth. The actual properties are also introduced at the inner boundary of the CORHEL model and the simulated solar wind disturbances near the Earth agree with the in situ observation of the solar wind disturbances associated with the 13 December 2006 frontside full-halo CME.

Thus we suggest that both the mathematical relationship between the apparent and actual kinematic properties established here and the minimum distance assumption used in the one-point approach for determining the projection angle are valid for fast frontside full-halo CMEs. We are examining more events to further validate the one-point approach.

Finally, the limitation of the circular cone model in inverting model parameters should be emphasized. As shown in Zhao [2008], the model parameters obtained using the elliptic cone model should be the same as those using the circular cone model if the elliptic halo is indeed formed by the projection of a circular cone base onto the sky-plane. The model parameters β and R_c (ω_y and ω_z) inverted by the elliptic cone model are, however, significantly greater (less) than those by the circular cone model (see Table 1), though the minor-axis of the 13 december 2006 halo CME passes close to the solar disk center. It indicates that the condition of passing through the solar disk center of the minor axis is only a necessary condition, but not a sufficient condition for using the circular cone model to invert model parameters. The significant difference is understandable. In the case of $\chi \sim 0$, we have $SA_{xh} = SA_{zb} \sin\beta$ and $SA_{yh} = SA_{yb}$. By using the circular cone model means assuming $SA_{zb} = SA_{yb} = SA_{yh}$ so that we have $\sin\beta = SA_{xh}/SA_{yh}$. In fact, for the 13 december 2006 full-halo CME $SA_{zb} = R_c \tan\omega_z = 4.17$ Rs, and $SA_{yb} = R_c \tan\omega_y = 4.46$ Rs. Here $SA_{yh} = SA_{yb}$ but $SA_{yh} > SA_{zb}$. Thus the parameter β obtained by $\sin\beta = SA_{xh}/SA_{yh}$ that is valid for the circular cone model is $\sim 10^\circ$ less than the real one, though the difference between ω_y and ω_z is only 2°. To avoid any misuse of the circular cone model, the elliptic cone model is strongly advised for inverting the model parameters for all kinds of frontside full-halo CMEs.

6. acknowledgments

We thank Dr. Ying Liu for sending us his preprint on the estimate of the radial propagation speed using Type II observation for the 13 December 2006 event. This work is supported by NASA grants NAGW 2502 and NAG5-3077, by NSF grant ATM9400298.

References

Case, A.W., Spence, H.E., Owens, M.J., Riley, P. and D. Odstrcil, The ambient solar wind?s e?ect on ICME transit times, *Geophys. Res. Lett.*, in press, 2008.

Cremades, H., Three-dimensional configuration and evolution of coronal mass ejections, Ph. D. thesis, Copernicus GmbH, Katlenburg-Lindau, Germany, ISBN: 3-936586-40-3, 2005.

Cremades, H. and V. Bothmer, Geometrical properties of coronal mass ejections, in *Proc. IAL symp. 226 on Coronal and Stellar Mass Ejections*, eds. K. P. Dere, J. Wang, and Y. Yan, 48, 2005.

Cremades, H. and V. Bothmer, Tripathi, D., Properties of Structured Coronal Mass Ejections in Solar Cycle 23, *Adv. Space Res. 38*, 3, 461-465, 2006.

Gopalswamy, N., A. Lara, S. Yashiro, S. Nunes, and R. A. Howard, Coronal mass ejection activity during solar cycle 23, in *Proc. ISCS 2003 Symposium on Solar Variability as an Input to Earth's Environment*, ESA-SP 535, p. 403, 2003.

Gopalswamy, N., S. Yashiro, and S. Akiyama, Geoeffectiveness of halo coronal mass ejections, Journal Geophys. Res., *in press,*, 2007.

Howard, R. A., D. J. Michels, N. R. Sheeley Jr., and M. J. Koomen, The observation of a coronal transient directed at earth, *Astrophys. J., 263,* l101, 1982.

Linker, J., et al., Magnetohydrodynamic modeling of the solar corona during whole sun month, *J. Geophys. Res., 104*, 9809-9830, 1999.

Liu, Y., J. G. Luhmann, R. Müller-Mellin, P. C. Schroeder, L. Wang, R. P. Lin, S. D. Bale, Y. Li, M. H. Acuña, and J.-A. Sauvaud, A Comprehensive View of the 2006 December 13 CME: From the Sun to Interplanetary Space, *Astrophys. J.*, Accepted, 2008.

Mikic, Z., J. A. Linker, D. D. Schnack, R. Lionello, and A. Tarditi, Magnetohydrodynamic modeling of the global solar corona, *Phys. Plasma, 6*, 2217, 1999.

Odstrcil, D., Modeling 3-D solar wind structures, *Adv. Space Res., 32*, 497-506, 2003.

Odstrcil, D., V. Pizzo, J. A. Linker, P. Riley, R. Lionello, and Z. Mikic, Initial coupling of coronal and heliospheric numerical magnetohydrodynamic codes, *J. Atmos. Solar Terr. Phys., 66*, 1311-1320, 2004a.

Odstrcil, D., P. Riley, and X.-P. Zhao, Numerical simulation of the 12 May 1997 interplanetary CME event, *J. Geophys. Res., 109*, doi:10.1029/2003JA010135, 2004b.

Owens, M. J., H. E. Spence, S. McGregor, W. J. Hughes, J. M. Quinn, C. N. Arge, P. Riley, J. Linker, and D. Odstrcil, Metrics for solar wind prediction models: Comparison of empirical, hybrid and physics-based schemes with 8-years of l1 observations, *Space Wea. J., 6*, S08001 10.1029/2007SW000380, 2008.

Plunkett, S. P., et al., Solar source regions of coronal mass ejections and their geomagnetic effects, *J. Atmos. Sol. Terr. Phys., 63*, 389, 2001.

Riley, P., C. Schatzman, H. V. Cane, I. G. Richardson, N. Gopalswamy, On the rates of coronal mass ejections: remote solar and in situ observations, *Astrophys. J., 647*, 648, 2006.

Xie, H., L. Ofman and G. Lawrence, Cone model for halo cmes: application to space weather forecasting, Journal Geophys. Res., *109*, A03109, doi:10.1029/2003ja010226, 2004.

Zhao, X. P., Determination of geometrical and kinematic properties of frontside halo coronal mass ejections, in *Proc. IAL symp. 226 on Coronal and Stellar Mass*

Ejections, eds. K. P. Dere, J. Wang, and Y. Yan, 42, 2005.

Zhao, X. P., Inversion solutions of the elliptic cone model for disk frontside full halo coronal mass ejections, Journal Geophys. Res., *113*, A02101, doi:10.1029/2007JA012582, 2008.

Zhao, X. P., S. P. Plunkett and W. Liu, Determination of geophysical and kinematic properties of halo coronal mass ejections using the cone model, Journal Geophys. Res., *107*, No A8, doi:10.1029/2001JA009143, 2002

Zhao, X. P. and D. F. Webb, Source regions and storm effectiveness of frontside full halo coronal mass ejections, Journal Geophys. Res., *108*, 1234, doi:10.1029/2002JA009606, 2003.

X. P. Zhao, W. W. Hansen Experimental Physics Laboratory, Stanford University, Stanford, CA 94305-4085. (e-mail:xuepu@sun.stanford.edu)

Received ________________________

This manuscript was prepared with AGU's LaTeX macros v5, with the extension package 'AGU^{++}' by P. W. Daly, version 1.6b from 1999/08/19.

Figure Captions

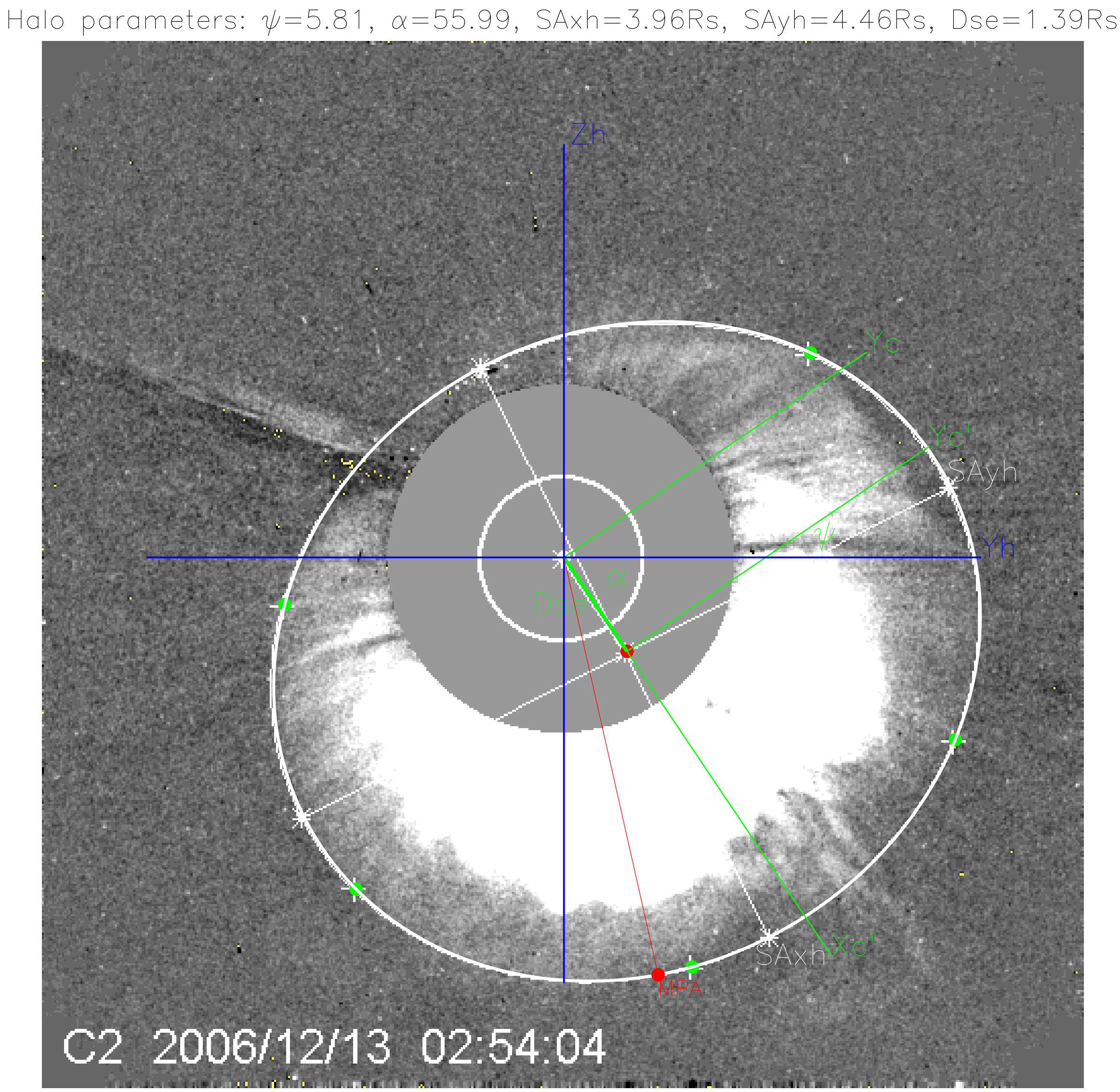

Figure 1. The definition and values of five halo parameters (SA_{xh}, SA_{yh}, ψ, D_{se}, α) for the 13 December 2006 frontside full-halo CME. Here X_c' and Y_c' are, respectively, aligned with and perpendicular to the direction from the solar disk center to the halo center, D_{se} (the short thick green line). Parameters ψ and α denote the angles between SA_{yh} and Y_c' and between X_c' and Y_h, respectively.

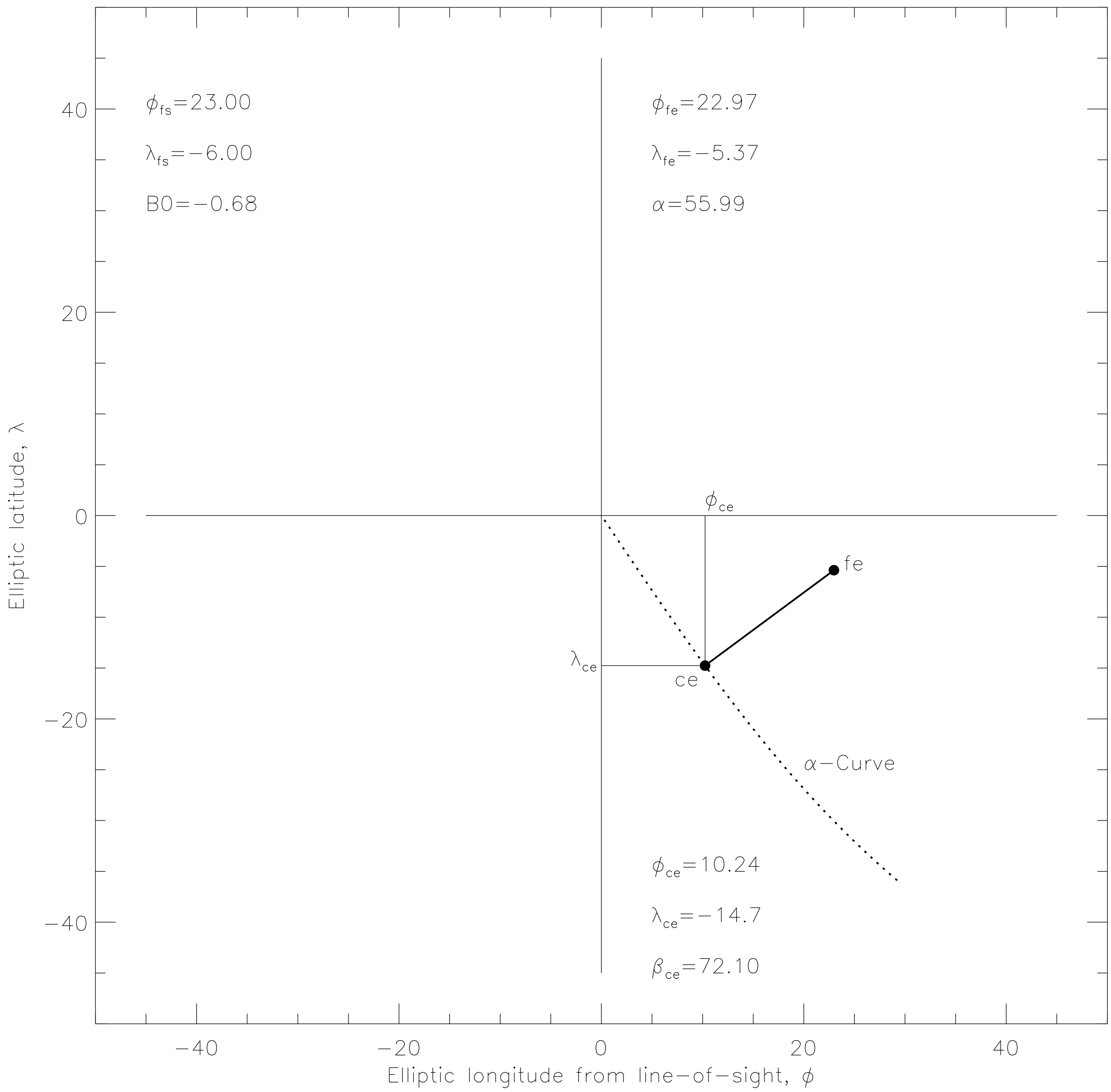

Figure 2. Description of the one-point approach for finding out the CME propagation direction (ϕ_{ce},λ_{ce}) or β on the basis of halo parameter α and the location of CME-associated flare (ϕ_{fs},λ_{se}). See text for details.

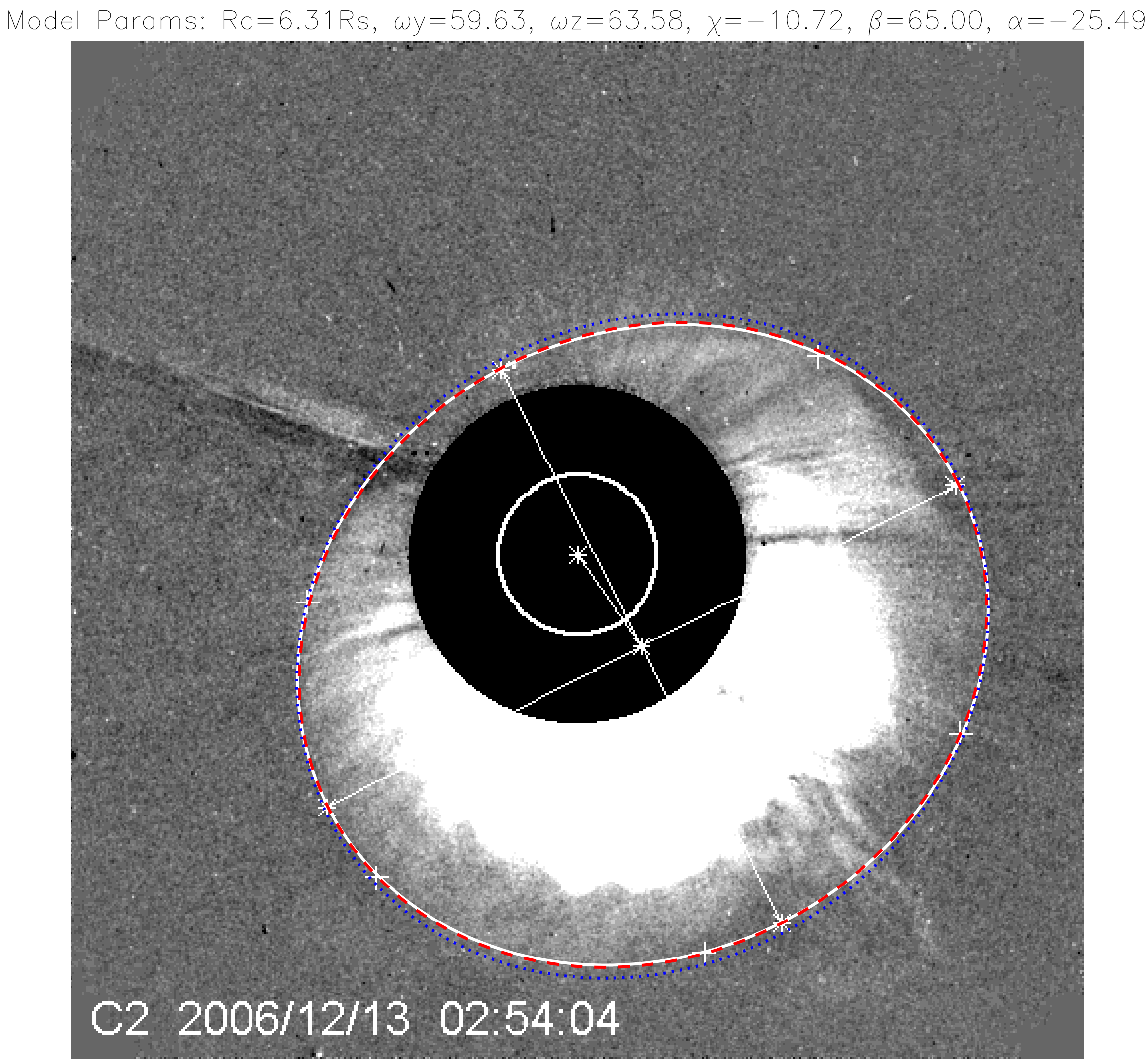

Figure 3. Comparison of the modeled halos by the elliptic cone model (Red dashed ellipse) and the cone model (Blue dotted ellipse) with the observed one (White solid ellipse). Both modeled halos agree with the observed one well.

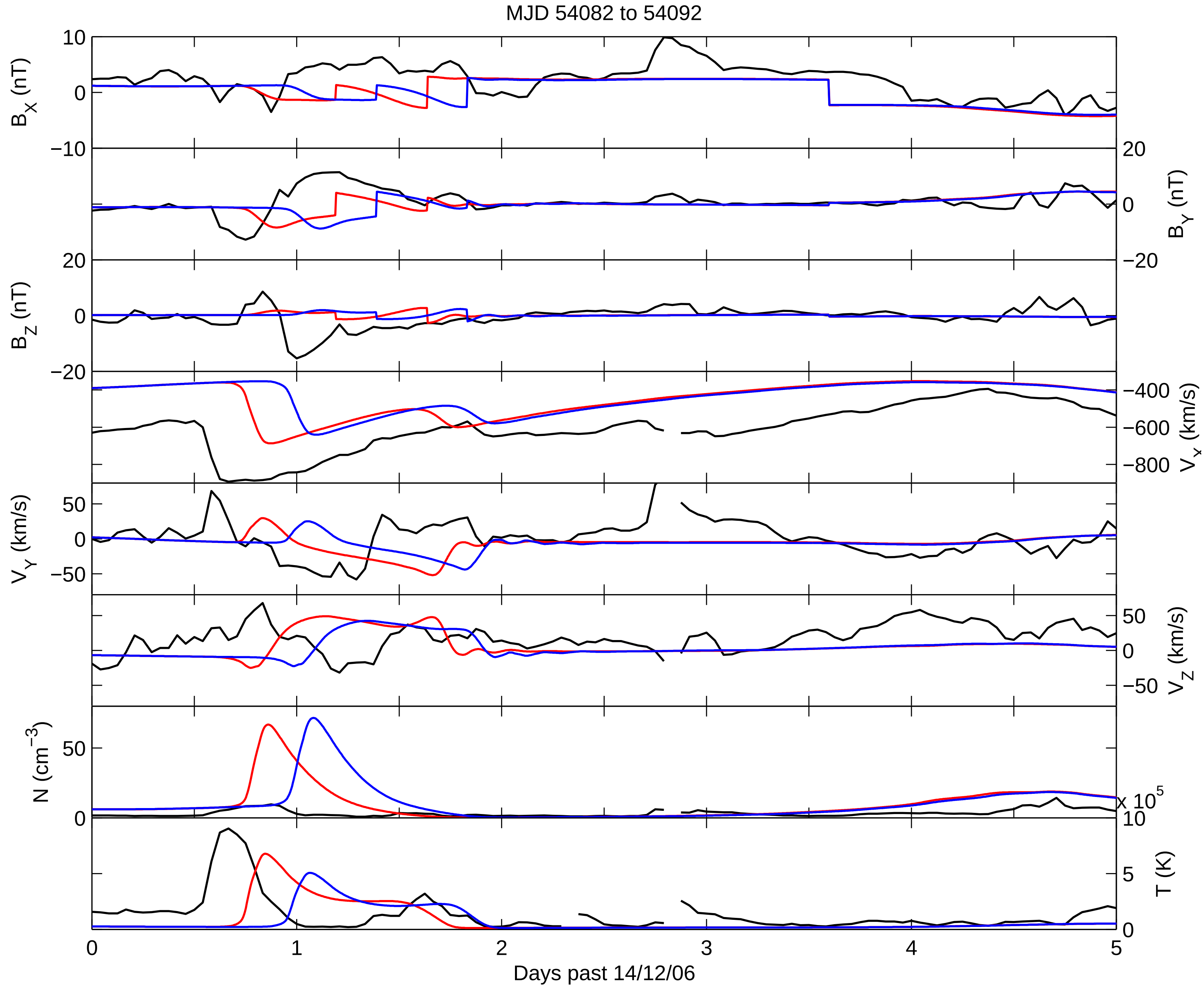

Figure 4. Comparison of simulated near-Earth solar wind disturbances initiated with elliptic (red) and circular (blue) cone model fits to the 13 December 2006 FFH CME observations to the ACE-observed near-Earth solar wind profile (black).

Tables

Table 1. Given Parameters and Model Parameters

Given parameters	Model parameters	Elliptic cone model	Cone model
Flare λ=-6°	CME λ	-14.70°	-22.41°
Flare ϕ=23°	CME ϕ	10.24°	16.16°
α=55.99°	α	55.99°	55.99°
	β	72.10°	62.62°
D_{se}=1.39Rs	R_c	4.53Rs	3.02Rs
SA_{xh}=3.96Rs	ω_y	44.61°	55.88°
SA_{yh}=4.46Rs	ω_z	42.64°	55.88°
ψ=5.81°	χ	5.97°	0.0°
MPA=193°	δ_b	250°	245°
V_{es1}=1774km/s	V_{er1}	2064km/s	1795km/s
V_{es2}=1930km/s	V_{er2}	2245km/s	1953km/s
a_{es}=-61.4m/s^2	a_{er}	-71.48m/s^2	-62.16m/s^2
	$V_{er2_{01}}$	2323km/s	1997km/s
	$V_{er2_{30}}$	1585km/s	1217km/s